Geometrically motivated set-point control strategy for the standard N-trailer vehicle

The paper presented during IEEE 2011 Intelligent Vehicles Symposium, pp. 138-143, Baden-Baden, Germany, June 5-9, 2011. ©2011 IEEE

Maciej Michałek

***Abstract*— The paper presents a novel control strategy for the problem of set-point feedback control for an articulated vehicle consisting of the unicycle-like tractor followed by the N passive semi-trailers. The concept results from geometrical interpretations of the vehicle model and the way in which the velocity components propagate along the kinematic chain. The control strategy is formulated for the original vehicle configuration space not involving any model transformations or approximations. The solution proposed is characterized by the fast and non-oscillatory convergence of the vehicle to the desired configuration. Formal considerations are examined by the simulations of backward parking maneuvers with 3-trailer vehicle, where the control input limitations of the tractor are preserved by using a simple scaling procedure.**

I. Introduction

The set-point control for restricted-mobility robots equipped with trailers is especially demanding. Difficulties result from nonholonomic nature of the robot kinematics with a less number of control inputs in comparison to a number of controlled variables, from singularities of its kinematic chain [2], and from its structural instability in a form of *folding effect* during backward motion.

In this paper we consider a problem of set-point control design for an articulated vehicle composed of the unicycle-like tractor followed by N passive trailers hooked at a mid-point of a preceding wheel-axle (see Fig. 1a)). This vehicle has been called in [10] the *standard N-trailer* system; its controllability was proved in [4]. The structure of the N-trailer system can be treated as an equivalent kinematic skeleton of many practical vehicles, while the set-point control task corresponds to the parking maneuvers. Since the parking maneuvers for vehicles with trailers are the involving duties of transportation vehicle drivers in their everyday work, automation of these tasks seems to be practically justified and desirable [14].

Feedback stabilization for the standard N-trailer vehicle was treated in the literature in the last two decades by several authors using different approaches, for example: smooth time-varying control [11], homogeneous and hybrid feedbacks [6], [9], transverse function method [7], and fuzzy logic concept [13]. Most solutions presented in the literature have been presented for the chained-form approximation of the original vehicle kinematics [12]. These results are very elegant and general, but suffer from their intrinsic locality (see [8]), which can be limiting in practical applications, and can lead to unacceptable control quality in the original task space [6].

The objective of this work is to present an alternative approach to the set-point control task for the standard N-trailer system. In the article the control law is derived using intuitive and geometrically motivated arguments formulated, in contrast to many existing solutions, in the original configuration space of the vehicle. Control formulation does not require any model transformation or approximation. The resultant cascaded control law is simple, with clearly interpretable components and straightforward tuning, and it leads to the non-oscillatory vehicle motion in the task space. Although a formal stability proof of the control system still remains an open problem, the simulation results obtained togehter with the preliminary analysis of the closed-loop system dynamics sketched in Section V seem to be promising.

II. Vehicle kinematics and the control problem

Articulated vehicle under consideration is schematically presented in Fig. 1a). It consists of $N+1$ segments: the first one is a unicycle-like tractor (active segment) followed by N semi-trailers (passive segments) of the length $L_i > 0,\ i = 1, \dots, N$ – everyone hitched with a passive joint located exactly on the axle mid-point of a preceding segment. Configuration of the vehicle can be represented by the vector $\boldsymbol{q} = [\beta_1\ \dots\ \beta_N\ \theta_N\ x_N\ y_N]^T \in \mathbb{R}^{N+3}$ with clear geometrical interpretation resulting from Fig. 1. Position of the last-trailer $\overline{\boldsymbol{q}}^* = [x_N\ y_N]^T \in \mathbb{R}^2$, taken as a subvector of its posture $\overline{\boldsymbol{q}} = [\theta_N\ x_N\ y_N]^T \in \mathbb{R}^3$, represents the *guidance point* P of the vehicle used in the control problem formulation in Section II-B. The only control inputs of the vehicle $\boldsymbol{u}_0 = [\omega_0\ v_0]^T \in \mathbb{R}^2$ are the angular ω_0 and longitudinal v_0 velocities of the tractor.

A. Basic kinematic relationships

Let us formulate kinematics of the vehicle in a manner useful for subsequent control development. In this formulation every i-th segment ($i = 0, 1, 2, 3 \dots$) of the vehicle kinematic chain from Fig. 1a) can be described by the unicycle model

$$\dot{\theta}_i = \omega_i, \tag{1}$$

$$\dot{x}_i = v_i \cos\theta_i, \tag{2}$$

$$\dot{y}_i = v_i \sin\theta_i, \tag{3}$$

where for $i = 0$ one obtains the tractor kinematics with control inputs ω_0 and v_0. For $i = 1, 2, 3 \dots$ the fictitious

This work is supported by the Polish scientific fund in years 2010-2012 as the research project No. N N514 087038.

The author is with Chair of Control and Systems Engineering, Poznan University of Technology, Piotrowo 3A, 60-965 Poznań, Poland maciej.michalek@put.poznan.pl

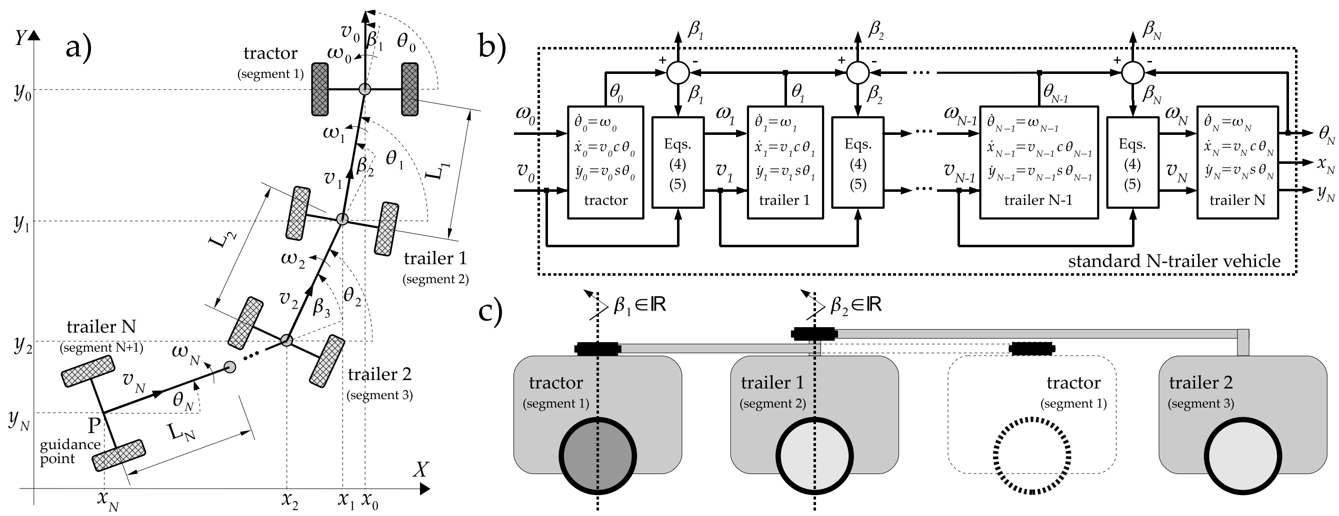

Fig. 1. Subfigure a): the standard N-trailer vehicle in a global frame. Subfigure b): schematic diagram of the N-trailer vehicle kinematics with inputs ω_0, v_0 and configuration vector $\boldsymbol{q}$. Subfigure c): the two-trailer vehicle with mechanical structure permitting for unbounded rotation in the joints ($\beta_1, \beta_2 \in \mathbb{R}$).

control inputs ω_i, v_i of the i-th trailer result from the following recurrent equations:

$$\omega_i = \frac{1}{L_i} v_{i-1} \sin\beta_i, \tag{4}$$

$$v_i = v_{i-1} \cos\beta_i \tag{5}$$

with the i-th joint angle

$$\beta_i = \theta_{i-1} - \theta_i. \tag{6}$$

Equations (4)-(6) describe how the physical inputs ω_0 and v_0 propagate to the i-th trailer along the vehicle kinematic chain. This is clarified by the schematic diagram in Fig. 1b), which illustrates the N-trailer vehicle kinematic model in the above interpretation. Combining (1) to (6) one can write the closed-form kinematics of the articulated vehicle with the selected configuration vector $\boldsymbol{q}$ and with the tractor input $\boldsymbol{u}_0$ leading to the driftless control system $\dot{\boldsymbol{q}} = \boldsymbol{S}(\boldsymbol{q})\boldsymbol{u}_0$ with $\boldsymbol{S}(\boldsymbol{q}) \in \mathbb{R}^{(N+3)\times 2}$ being an appropriate kinematic matrix [2]. Since the closed-form model does not provide key geometrical insights used in the control development further proposed, we will utilize its recurrent form (1)-(6).

B. Control problem statement

Since the guidance point P, represented by the vector $\overline{\boldsymbol{q}}^* = [x_N \ y_N]^T$, has been situated on the last trailer, the control task will be formulated with a special attention paid for the last vehicle segment. It can be justified by practical applications where the task performed by the vehicle is directly related to the last trailer. Let us define the reference configuration of the vehicle

$$\boldsymbol{q}_t = [\beta_{t1} \ \ldots \ \beta_{tN} \ \theta_{tN} \ x_{tN} \ y_{tN}]^T \in \mathbb{R}^{N+3}$$

with $\beta_{ti} \triangleq 0$, $i = 1, \ldots, N$, and the configuration error:

$$\boldsymbol{e} = \begin{bmatrix} \boldsymbol{e}_\beta \\ \overline{\boldsymbol{e}} \end{bmatrix} = [e_{\beta 1} \ \ldots e_{\beta N} \ e_\theta \ e_x \ e_y]^T \triangleq \boldsymbol{q}_t - \boldsymbol{q}, \tag{7}$$

with the joint angle error component

$$\boldsymbol{e}_\beta \triangleq [\beta_{t1} - \beta_1 \ \ldots \ \beta_{tN} - \beta_N]^T \in \mathbb{R}^N \tag{8}$$

and the posture error component

$$\overline{\boldsymbol{e}} = \begin{bmatrix} e_\theta \\ e_x \\ e_y \end{bmatrix} \triangleq \overline{\boldsymbol{q}}_t - \overline{\boldsymbol{q}} = \begin{bmatrix} \theta_{tN} - \theta_N \\ x_{tN} - x_N \\ y_{tN} - y_N \end{bmatrix} \in \mathbb{R}^3. \tag{9}$$

Assuming that:

A1. the initial posture error $\overline{\boldsymbol{e}}(0) \neq \boldsymbol{0}$,
A2. all components of the configuration $\boldsymbol{q}$ are measurable,
A3. all the vehicle kinematic parameters L_i are known,

the control problem is to design a feedback control law $\boldsymbol{u}_0 = \boldsymbol{u}_0(\boldsymbol{q}_t, \boldsymbol{q}, \cdot)$ which applied to the vehicle kinematics represented by (1)-(6) makes the error (7) convergent in the sense that:

$$\lim_{\tau\to\infty} \|\overline{\boldsymbol{e}}(\tau)\| = 0 \quad \text{and} \quad \lim_{\tau\to\infty} e_{\beta i}(\tau) = \pm n\pi, \tag{10}$$

with τ denoting the time variable, and $n \in \{0, 1, 2, \ldots\}$.

According to the conditions imposed in (10), the defined control problem is more restrictive for the posture component of a last trailer than for the joint angle error of a kinematic chain. For $n > 0$ in the right-hand side limit of (10) one permits the vehicle to fold in joints when the last trailer approaches the reference posture $\overline{\boldsymbol{q}}_t$. At the first look one can find it an impractical case. However, in Fig. 1c) the two-trailer vehicle structure is presented which is designed in a way where all the joint angles can be changed without mechanical limits permitting the folding effect. Of course, higher number of trailers in the chain will make the mechanical design more problematic and possibly less practical. Thus, to show and compare different possibilities of control problem solution, we will provide two versions of the control law: the first one permitting $n > 0$ in (10) with unbounded domain for the joint angles (folding effect permitted), and the second one for $n = 0$ in (10) avoiding the folding effect and leading to straightening the vehicle kinematic chain in the neighborhood of $\overline{\boldsymbol{e}} = \boldsymbol{0}$.

III. Feedback control strategy

The general control strategy for articulated vehicle is a direct consequence of equations (4)-(5) which describe propagation of tractor velocities to particular trailers along the vehicle kinematic chain. To explain the concept let us begin from the last trailer where the guidance point P has been selected. Let us make a thought experiment where the N-th trailer is temporarily separated from the remaining vehicle chain and can be treated as the unicycle-like vehicle with control inputs ω_N, v_N (cf. Fig. 1b)). Furthermore, assume that the feedback control functions $\omega_N := \Phi_\omega(\overline{e}, \cdot)$, $v_N := \Phi_v(\overline{e}, \cdot)$ which guarantee asymptotic convergence of the posture $\overline{q}$ of the unicycle model (1)-(3) with $i := N$ to the desired posture $\overline{q}_t$ are given. We do not define these functions in detail now, it will be done in Section III-B.

In order to formulate the control strategy we need to answer the question how can one execute the feedback functions $\Phi_\omega(\overline{e}, \cdot)$ and $\Phi_v(\overline{e}, \cdot)$ in the case when the N-th trailer is not directly driven by ω_N, v_N, but it is passively linked to the kinematic chain driven only by the tractor. Although the N-th trailer cannot be directly driven, one can make the $(N-1)$-st trailer move in a way which forces the desired control action determined by functions $\Phi_\omega(\overline{e}, \cdot)$ and $\Phi_v(\overline{e}, \cdot)$ on the N-th trailer. Relations (4)-(5) reveal how to obtain it using the fictitious input v_{N-1} of the $(N-1)$-th trailer and the joint angle β_N. Proceeding analogous reasoning for the subsequent vehicle segments along the whole kinematic chain (where the $(i-1)$-st segment influences motion of the i-th one), one can derive the control law for the physically available tractor inputs ω_0, v_0, which allow accomplish desired motion of the last trailer (*guiding* segment). The above concept will be formalized next.

A. Control strategy permitting the folding effect

Let us denote by ω_{di-1} and v_{di-1} the desired fictitious inputs which the $(i-1)$-st vehicle segment should be forced with in order to execute the desired motion of the i-th segment. Simple combination of relations (4)-(5) yields the equations which determine the desired longitudinal velocity v_{di-1} and the desired i-th joint angle:

$$v_{di-1} \triangleq L_i \omega_{di} \sin\beta_i + v_{di}\cos\beta_i, \tag{11}$$

$$\beta_{di} \triangleq \text{Atan2c}\left(L_i\omega_{di}\cdot v_{di-1}, v_{di}\cdot v_{di-1}\right) \in \mathbb{R}, \tag{12}$$

where $\text{Atan2c}(\cdot,\cdot) : \mathbb{R}\times\mathbb{R} \mapsto \mathbb{R}$ is a continuous version of the four-quadrant function $\text{Atan2}(\cdot,\cdot) : \mathbb{R}\times\mathbb{R} \mapsto (-\pi, \pi]$ (it has been introduced to ensure continuous domain for β_{di} variables[1]). The term v_{di-1} used in (12) determines the appropriate sign of the two function arguments. Now the angular fictitious input ω_{di-1} remains to be determined. To do this, let us differentiate (6) and use (1) to obtain

$$\dot{\beta}_i = \omega_{i-1} - \omega_i =: \nu_i. \tag{13}$$

The above equation may suggest how to define ν_i to ensure that the auxiliary joint angle error

$$e_{di} \triangleq (\beta_{di} - \beta_i) \in \mathbb{R} \tag{14}$$

will converge to zero implying that the desired angle (12) is realized by the $(i-1)$-st vehicle segment. By taking in

[1]More details how to compute $\text{Atan2c}(\cdot,\cdot)$ function can be found in [1].

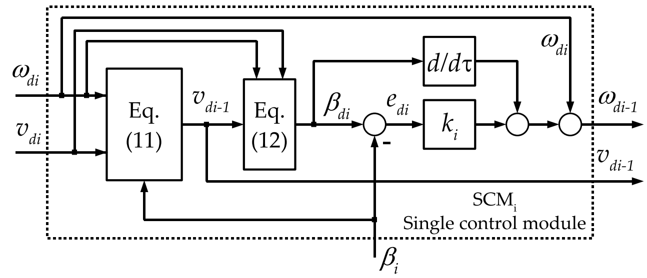

Fig. 2. Block schema of the i-th Single Control Module (SCM$_i$).

(13) the definition $\nu_i \triangleq k_i e_{di} + \dot{\beta}_{di}$ with $k_i > 0$ and $\dot{\beta}_{di} \equiv d\beta_{di}/d\tau$, one gets the differential equation $\dot{e}_{di} + k_i e_{di} = 0$. This implies the exponential convergence $e_{di}(\tau) \to 0$ as $\tau \to \infty$. Now, the desired angular velocity for the $(i-1)$-st vehicle segment can be defined according to (13) as follows:

$$\omega_{di-1} \triangleq \nu_i + \omega_{di} \triangleq k_i e_{di} + \dot{\beta}_{di} + \omega_{di}, \tag{15}$$

where $k_i > 0$ is now a control design coefficient, and $\dot{\beta}_{di}$ plays a role of the feed-forward term.

Three definitions (11), (12), and (15) constitute the i-th Single Control Module (SCM$_i$) presented by the schematic diagram in Fig. 2 with the feedback from the joint angle β_i. Serial connections of SCM$_i$ blocks allows propagating the computations of desired velocities between arbitrary number of vehicle segments. The recurrent relations formulated in (11), (12), and (15) can be iterated from $i = N$ to $i = 1$, starting from the last trailer by taking $\omega_{dN} := \Phi_\omega(\overline{e}, \cdot)$, $v_{dN} := \Phi_v(\overline{e}, \cdot)$ and finishing on the tractor segment obtaining the control inputs $\omega_0 := \omega_{d0}(\cdot)$, $v_0 := v_{d0}(\cdot)$. The resultant equations of the feedback controller for the standard N-trailer vehicle can be formulated as follows:

$$v_{dN} := \Phi_v(\overline{e}, \cdot) \tag{16}$$

$$\omega_{dN} := \Phi_\omega(\overline{e}, \cdot) \tag{17}$$

$$v_{dN-1} := L_N\omega_{dN}\sin\beta_N + v_{dN}\cos\beta_N \tag{18}$$

$$\beta_{dN} := \text{Atan2c}\left(L_N\omega_{dN}\cdot v_{dN-1}, v_{dN}\cdot v_{dN-1}\right) \tag{19}$$

$$\omega_{dN-1} := k_N(\beta_{dN} - \beta_N) + \dot{\beta}_{dN} + \omega_{dN} \tag{20}$$

$$\vdots$$

$$v_{d1} := L_2\omega_{d2}\sin\beta_2 + v_{d2}\cos\beta_2 \tag{21}$$

$$\beta_{d2} := \text{Atan2c}\left(L_2\omega_{d2}\cdot v_{d1}, v_{d2}\cdot v_{d1}\right) \tag{22}$$

$$\omega_{d1} := k_2(\beta_{d2} - \beta_2) + \dot{\beta}_{d2} + \omega_{d2} \tag{23}$$

$$v_0 = v_{0d} := L_1\omega_{d1}\sin\beta_1 + v_{d1}\cos\beta_1 \tag{24}$$

$$\beta_{d1} := \text{Atan2c}\left(L_1\omega_{d1}\cdot v_{d0}, v_{d1}\cdot v_{d0}\right) \tag{25}$$

$$\omega_0 = \omega_{d0} := k_1(\beta_{d1} - \beta_1) + \dot{\beta}_{d1} + \omega_{d1}, \tag{26}$$

where equations (24) and (26) describe direct application of the control inputs to the vehicle tractor. Figure 3 illustrates the structure of the resultant cascaded control system. Note that the controlled output of the articulated vehicle is the last trailer posture $\overline{q} \in \mathbb{R}^3$, while the angles β_1 to β_N are the auxiliary outputs.

The Last-Trailer Posture Stabilizer (LTPS) block in Fig. 3 represents a stabilizer designed for the unicycle kinematics of the last trailer. This block computes the feedback control

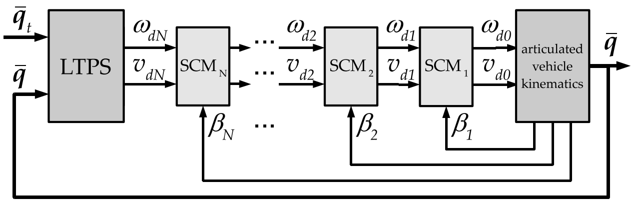

Fig. 3. Block schema of the proposed cascaded feedback control system for the standard N-trailer vehicle. The controller consists of the Single Control Modules (SCM_1 to SCM_N) connected in series, and the Last-Trailer Posture Stabilizer (LTPS) block dedicated for the last trailer treated as the unicycle.

functions $\Phi_\omega(\overline{e}, \cdot)$ and $\Phi_v(\overline{e}, \cdot)$ used in equations (16)-(17). From now on we assume that the feedback functions Φ_v and Φ_ω are determined by the VFO stabilizer introduced in [1] and briefly recalled in the next subsection.

B. Last-Trailer Posture Stabilizer – the VFO controller

The Vector-Field-Orientation (VFO) stabilizer results from simple geometrical interpretations related to the unicycle kinematics (1)-(3). Selection of the VFO stabilizer for the LTPS block has been motivated by the specific and practically useful features of the VFO closed-loop system, where the fast and non-oscillatory convergence together with the so-called *directing effect* can be observed. Since [1] includes detailed description of the VFO method, let us only briefly recall equations of the stabilizer, written for the unicycle model of the last trailer, with short explanation of its particular terms.

The VFO controller can be formulated as follows:

$$\Phi_\omega \triangleq k_a e_a + \dot{\theta}_a, \qquad \Phi_v \triangleq h_x \cos\theta_N + h_y \sin\theta_N, \quad (27)$$

where Φ_ω is called the *orienting control*, and Φ_v the *pushing control*. Particular terms in the above definitions are determined in the following way:

$$h_x = k_p e_x + v_x, \quad v_x = -\eta\sigma\sqrt{e_x^2 + e_y^2}\cos\theta_{tN}, \quad (28)$$

$$h_y = k_p e_y + v_y, \quad v_y = -\eta\sigma\sqrt{e_x^2 + e_y^2}\sin\theta_{tN}, \quad (29)$$

$$e_a = \theta_a - \theta_N, \quad (30)$$

$$\theta_a = \text{Atan2c}\left(\sigma \cdot h_y, \sigma \cdot h_x\right), \quad (31)$$

$$\dot{\theta}_a = (\dot{h}_y h_x - h_y \dot{h}_x)/(h_x^2 + h_y^2), \quad (32)$$

where $k_a, k_p > 0$ and $\eta \in (0, k_p)$ are the design coefficients, and $\sigma \in \{-1, +1\}$ is the decision factor which allows designer to select the desired motion strategy: forward by taking $\sigma := +1$ or backward by taking $\sigma := -1$. Note that e_x and e_y are the components of posture error (9), and θ_{tN} is the reference orientation defined by the reference configuration $\boldsymbol{q}_t$ (cf. Section II-B). It was proved in [1] that the feedback control functions defined by (27) guarantee asymptotic convergence of error $\overline{e}(\tau)$ to zero if functions (27) are directly forced as inputs to the unicycle-like kinematics.

Functions defined by (27) can now be substituted into (16) and (17) yielding the complete set-point controller for the standard N-trailer vehicle, which allows solving the control problem stated in Section II-B.

C. Control strategy with folding effect avoidance

Control strategy presented so far admits vehicle folding in the joints. It is a consequence of definition (12), where the desired angles are the real variables. It may be limiting in a case of practical application. Thus to avoid the vehicle folding effect and obtain a solution for the control problem with $n = 0$ (cf. (10)) we propose to modify (11) as follows:

$$v_{di-1} \triangleq \sigma \left| L_i \omega_{di} \sin\beta_i + v_{di}\cos\beta_i \right|, \quad (33)$$

where σ is the decision factor introduced in (28)-(32) (inherited from the VFO stabilizer used in LTPS block). Other definitions remain unchanged. Note that by modification (33) and due to features of the VFO stabilizer (see [1]) the second argument of Atan2c $(\cdot, \cdot)$ function in (12) may now have a constant non-negative sign. As a consequence, the value-set of function Atan2c $(\cdot, \cdot)$ can be limited to the first and fourth quadrants. In the modified controller version equations (18), (21), and (24) have to be replaced by (33) using the appropriate indexes.

D. Comments on control implementation

The desired angles defined by (12) and their time-derivatives are undetermined at the time instants τ_I when the two arguments of Atan2c $(\cdot, \cdot)$ function are simultaneously equal to zero. One can cope with this problem using at τ_I the limit values β_{di}^- and $\dot{\beta}_{di}^-$, where $\beta_{di}^- = \lim_{\tau \to \tau_I^-} \beta_{di}(\tau)$ and $\dot{\beta}_{di}^- = \lim_{\tau \to \tau_I^-} \dot{\beta}_{di}(\tau)$, where τ_I^- directly precedes τ_I.

The time-derivatives $\dot{\beta}_{di}$, used in eqs. (20), (23), and (26), may be obtained by the formal differentiation of (12), but it requires the time-derivatives of signals ω_{di} and v_{di}. This may cause difficulties in practical implementation. Hence, we propose to use instead the so-called *exact robust differentiator* proposed for example in [5], or approximate the time-derivatives by their filtered versions $\dot{\beta}_{diF} = \mathcal{L}^{-1}\left\{s/(1 + sT_F)\right\}$, $T_F > 0$, which can be computed on-line numerically. In cases of slow vehicle motions the terms $\dot{\beta}_{di}$ can be even omitted in implementation, assuming however sufficiently high values of coefficients k_i to preserve stability of the closed-loop system.

One can formulate heuristic tuning rules for the proposed controller, which allows obtaining satisfactory results for the most cases. The first rule for the outer-loop VFO stabilizer (LTPS block) can be stated as follows: select $k_p \in (0; 5]$ as a compromise between the convergence rate and the noise-sensitivity, then choose $k_a := 2k_p$, and $\eta \in (0, k_p)$ according to the required intensity of the *directing effect* for the last trailer (the less the difference $k_p - \eta$, the greater intensity). Tuning rule for the inner loops (SCM blocks) recommends selection $k_i > k_{i+1}$, which results from the fact that attenuation of the last-trailer posture error requires increasingly sweeping maneuvers for the segments closer to the tractor.

E. Control input limitation

In practical implementation the control input $\boldsymbol{u}_0 = [\omega_0 \ v_0]^T$ computed according to Eqs. (24) and (26) should be post-processed in order to satisfy the velocity limits of the motors which drive the tractor wheels (the tractor is treated here as a differentially driven vehicle). Let us recall the simple scaling procedure which guarantees preserving the velocity limitations. By $\boldsymbol{\omega}_c = [\omega_{Rc}\ \omega_{Lc}]^T$ we denote the vector of desired tractor wheel velocities (right and left, respectively) computed as follows:

$$\boldsymbol{\omega}_c = \boldsymbol{J}^{-1}\boldsymbol{u}_{0c}, \qquad \boldsymbol{J} = \begin{bmatrix} r/b & -r/b \\ r/2 & r/2 \end{bmatrix}, \tag{34}$$

where r and b are the wheel radius and the wheel base of the tractor, respectively, and $\boldsymbol{u}_{0c} = [\omega_{0c}\ v_{0c}]^T$ is the *computed* control vector obtained according to (24) and (26). Let us define the strictly positive scaling function

$$s \triangleq \max\left\{1; \frac{|\omega_{Rc}|}{\omega_{w\max}}; \frac{|\omega_{Lc}|}{\omega_{w\max}}\right\}, \tag{35}$$

where $\omega_{w\max} > 0$ is the maximal admissible wheel velocity of the tractor. Now, the limited control input for the tractor is obtained as follows:

$$\boldsymbol{u}_0 = \boldsymbol{u}_{0c}/s. \tag{36}$$

The above scaling procedure is computed on-line and it ensures that the tractor wheel velocities do not exceeds $\pm\omega_{w\max}$ for all $\tau \geqslant 0$. Additionally, $\boldsymbol{u}_0(\tau)$ is parallel to $\boldsymbol{u}_{0c}(\tau)$ for all $\tau \geqslant 0$, which implies preservation of the instantaneous motion curvature of the tractor despite scaling of its input.

IV. Numerical validation

For the simulation purposes let us fix our attention to the 3-trailer vehicle. For $N = 3$ the VFO feedback functions (27) and equations (28)-(32) are related to the third trailer.

Effectiveness of the proposed set-point controller is illustrated by the results of two simulation tests presenting the so-called *parallel parking maneuvers*. The first simulation test (denoted as SF) reveals the vehicle folding effect due to usage of definition (11). In the second test (denoted as SnF) the folding effect has been avoided by utilization of definition (33) instead of (11). For the two simulations the following conditions and numerical values have been selected: $\boldsymbol{q}_t = [0\ 0\ 0\ \frac{\pi}{2}\ -1\ 0]^T$, $\boldsymbol{q}(0) = [0\ 0\ 0\ \frac{\pi}{2}\ 1\ 0]^T$, $L_1 = L_2 = L_3 = 0.25\,\mathrm{m}$, $k_1 = 50$, $k_2 = 30$, $k_3 = 5$, $k_a = 2$, $k_p = 1$, and $\eta = 0.8$, where $\boldsymbol{q}(0)$ denotes the vehicle initial configuration. The control strategy with backward motion for the last-trailer has been selected in both tests ($\sigma := -1$ in (28), (29), and (31)). For the sake of simplicity the feed-forward terms $\dot{\beta}_{d3}$ and $\dot{\beta}_{d2}$ have been omitted in the control implementation. Only the term $\dot{\beta}_{d1}$ has been approximated by its filtered version $\dot{\beta}_{d1F}$ using the filter time constant $T_F = 0.05\,\mathrm{s}$. The scaling procedure (34)-(36) has been utilized in both tests with $r = 0.025\,\mathrm{m}$, $b = 0.17\,\mathrm{m}$, and with the maximal admissible tractor wheel velocity $\omega_{w\max} = 8\pi\,\mathrm{rad/s}$. Results of the simulations are presented in Figs. 4-6. In Fig. 4 the last trailer is denoted by the red rectangle, while the tractor by the black triangle. Figs. 5-6 show the time plots of the last-trailer posture error components, the β-angles of the vehicle joints, and the amplitude-limited (scaled) control inputs of the tractor. The vehicle folding effect can be seen on the left plot in Fig. 4 where the folding occurs between the second and the third trailer. It is also confirmed by the center plot in Fig. 5, where β_3 angle converges to the value of $-\pi$. The lack of the folding effect is visible on the right plot in Fig. 4 and in the center plot in Fig. 6, where all β-angles converge to zero and do not approach the values of $\pm\pi$ during the whole control time-horizon.

V. Remarks and future works

The feedback controller presented in the paper comes from the geometrical arguments, thus stability of the closed-loop system has to be proved. Although stability and convergence issues still remain the open problems, the preliminary analysis conducted so far reveals promising features of the closed-loop dynamics. It can be shown that for the desired configuration $\boldsymbol{q}_t = \boldsymbol{0}$ the dynamics of the last-trailer posture error (9) and the auxiliary joint error $\boldsymbol{e}_d = [e_{d1}\ \ldots\ e_{dN}]^T$ take the form:

$$\dot{\overline{\boldsymbol{e}}} = \boldsymbol{f}(\overline{\boldsymbol{e}}) + \boldsymbol{f}_1(\overline{\boldsymbol{e}}, \boldsymbol{e}_d, \cdot), \qquad \dot{\boldsymbol{e}}_d = \boldsymbol{A}\boldsymbol{e}_d + \boldsymbol{f}_2(\overline{\boldsymbol{e}}, \boldsymbol{e}_d, \cdot),$$

where $\boldsymbol{f}_1(\overline{\boldsymbol{e}}, \boldsymbol{e}_d, \cdot) = \boldsymbol{G}(-\overline{\boldsymbol{e}})\boldsymbol{\Gamma}\boldsymbol{e}_{\omega v}(\overline{\boldsymbol{e}}, \boldsymbol{e}_d, \cdot)$, $\boldsymbol{G}(\cdot)$ is the unicycle kinematic matrix, $\boldsymbol{f}_2(\overline{\boldsymbol{e}}, \boldsymbol{e}_d, \cdot) = \boldsymbol{H}\boldsymbol{e}_{\omega v}(\overline{\boldsymbol{e}}, \boldsymbol{e}_d, \cdot)$, $\boldsymbol{e}_{\omega v} = [\boldsymbol{e}_\omega^T\ \boldsymbol{e}_v^T]^T$, $\boldsymbol{e}_\omega = [\omega_{d1} - \omega_1\ \ldots\ \omega_{dN} - \omega_N]^T$, $\boldsymbol{e}_v = [v_{d1} - v_1\ \ldots\ v_{dN} - v_N]^T$, $\boldsymbol{A} = \mathrm{diag}\{-k_i\}$ is Hurwitz, and $\boldsymbol{\Gamma}$ and $\boldsymbol{H}$ are the appropriate matrices with -1, 0, and $+1$ entries. Furthermore, one can show that $\boldsymbol{f}_2(\boldsymbol{e}_d = \boldsymbol{0}, \cdot) = \boldsymbol{0}$, $\boldsymbol{f}_1(\boldsymbol{e}_d = \boldsymbol{0}, \cdot) = \boldsymbol{0}$, and the nominal (unperturbed) dynamics $\dot{\overline{\boldsymbol{e}}} = \boldsymbol{f}(\overline{\boldsymbol{e}})$ is stable and asymptotically convergent (see the proof in [1]). We plan to proceed the further analysis using the stability theorems for interconnected dynamical systems, [3], showing first the required features of functions $\boldsymbol{f}_1(\cdot)$ and $\boldsymbol{f}_2(\cdot)$.

The control strategy proposed in the article consists of two main components: the serial chain of Single Control Modules (SCM$_i$ blocks), and the Last-Trailer Posture Stabilizer (LTPS block) – cf. Fig. 3. The chain of SCM$_i$ blocks has been derived independently from the LTPS block, thus the control scheme proposed seems to be more general in nature. Selection of the VFO stabilizer for the LTPS block can be found here as a special case justified by the geometrical characteristics of the VFO controller, which are beneficial in shaping the desired motion of the last trailer, and guaranteeing straightening the vehicle kinematic chain in the neighborhood of the set-point (see [1]). It seems that there is a possibility of a more general case where other alternative stabilizers can be applied for the LTPS block.

Experimental validation of the proposed control strategy on the laboratory-scale articulated vehicle with three trailers is planned in the near future. It will allow to practically examine robustness of the control system to violation of assumptions A2 and A3 stated in Subsection II-B, when the feedback measurements are noisy, and values of the kinematic parameters L_i are uncertain.

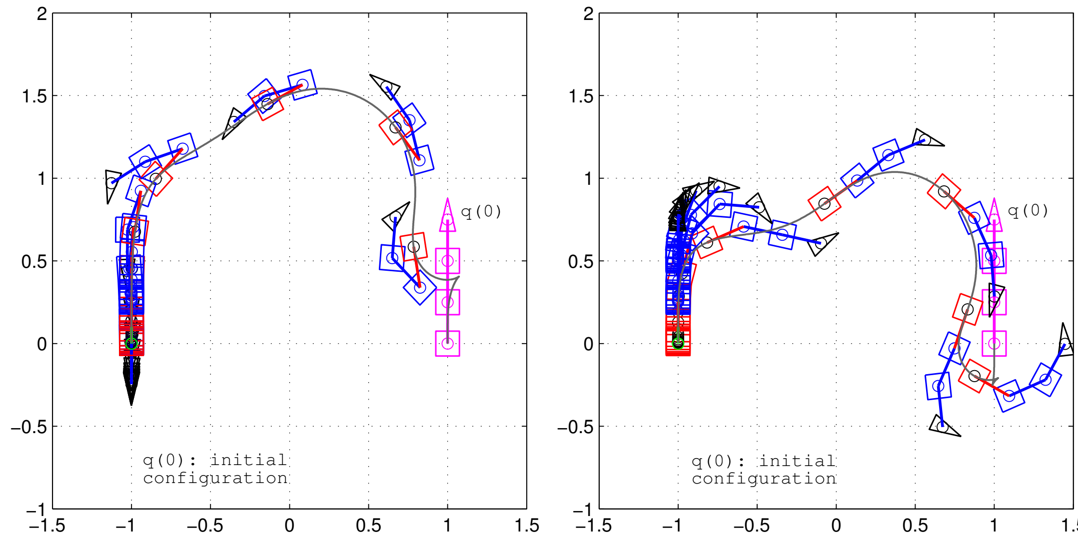

Fig. 4. The parking maneuvers in (x, y) plane (dimensions in [m]): with the vehicle folding effect (sim. SF – left) and without the folding effect (sim. SnF – right). Initial vehicle configuration is highlighted in magenta; the last trailer is denoted by the red rectangle, the tractor – by the black triangle.

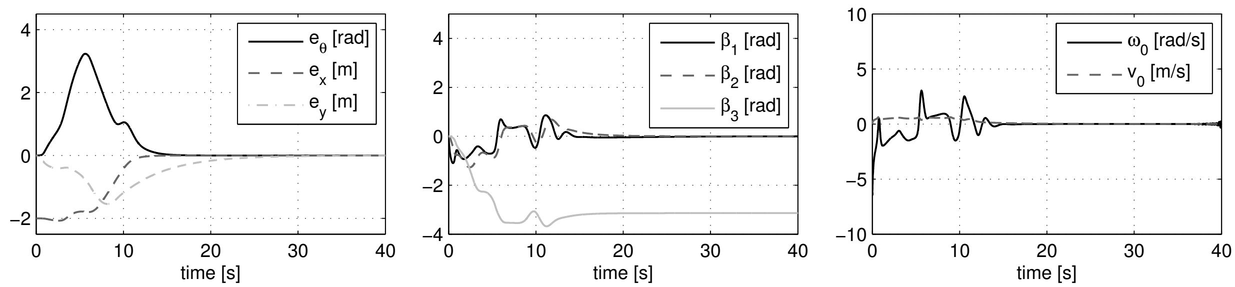

Fig. 5. Time plots of the last-trailer posture errors (left), the joint angles (center), and the scaled control inputs (right) for simulation SF.

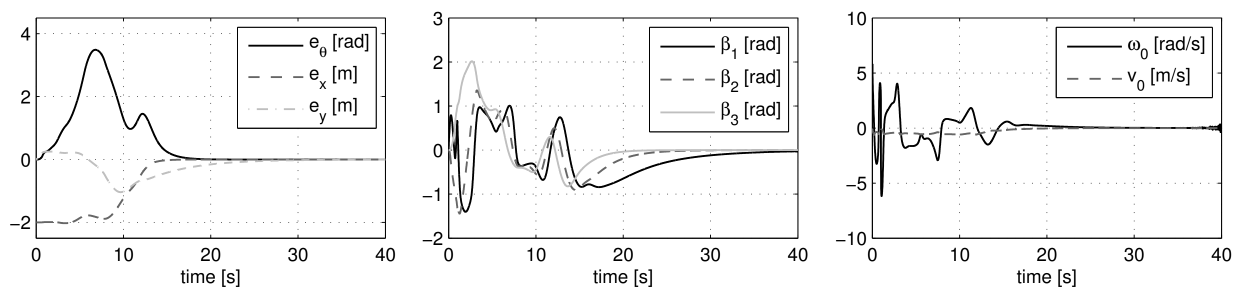

Fig. 6. Time plots of the last-trailer posture errors (left), the joint angles (center), and the scaled control inputs (right) for simulation SnF.

References

[1] M. Michałek and K. Kozłowski. Vector-Field-Orientation feedback control method for a differentially driven vehicle. *IEEE Transactions on Control Systems Technology*, 18(1):45–65, 2010.

[2] F. Jean. The car with N trailers: characterisation of the singular configurations. *Control, Opt. Calc. Variations*, 1:241–266, 1996.

[3] H. K. Khalil. *Nonlinear systems. 3rd Edition*. Prentice-Hall, Upper Saddle River, New Jersey, 2002.

[4] J. P. Laumond. Controllability of a multibody mobile robot. *IEEE Transactions on Robotics and Automation*, 9(6):755–763, 1993.

[5] A. Levant. Higher-order sliding modes, differentiation and output-feedback control. *Int. J. Control*, 76(9/10):924–941, 2003.

[6] R. T. M'Closkey and R. M. Murray. Experiments in exponential stabilization of a mobile robot towing a trailer. In *Proc. of the American Control Conference*, pages 988–993, Baltimore, USA, 1994.

[7] P. Morin and C. Samson. Transverse function control of a class of non-invariant driftless systems. Application to vehicles with trailers. In *Proceedings of the 47th IEEE Conference on Decision and Control*, pages 4312–4319, Cancun, Mexico, 2008.

[8] O. J. Sørdalen. Conversion of the kinematics of a car with n trailers into a chained form. In *Proc. IEEE Int. Conf. on Robotics and Automation*, pages 382–387, Atlanta, USA, 1993.

[9] O. J. Sørdalen and K. Y. Wichlund. Exponential stabilization of a car with n trailers. In *Proceedings of the 32th Conference on Decision and Control*, pages 978–983, San Antonio, USA, 1993.

[10] P. Rouchon, M. Fliess, J. Levine, and P. Martin. Flatness, motion planning and trailer systems. In *Proceedings of the 32nd Conference on Decision and Control*, pages 2700–2705, San Antonio, Texas, 1993.

[11] C. Samson. Control of chained systems. application to path following and time-varying point-stabilization of mobile robots. *IEEE Transactions On Automatic Control*, pages 64–77, 1995.

[12] O. J. Sørdalen and O. Egeland. Exponential stabilization of nonholonomic chained systems. *IEEE Transactions on Automatic Control*, 40(1):35–49, 1995.

[13] K. Tanaka, S. Hori, and H. O. Wang. Multiobjective control of a vehicle with triple trailers. *IEEE/ASME Trans. on Mechatronics*, 7(3):357–368, 2002.

[14] D. Zöbel. Trajectory segmentation for the autonomous control of backward motion for truck and trailer. *IEEE Trans. Intell. Transportation Systems*, 4(2):59–66, 2003.